Princeton Plasma Physics Laboratory

PPPL-5282

Adjoint method and runaway electron avalanche

C. Liu, D. Brennan, A. Bhattacharjee

August 2016

Prepared for the U.S. Department of Energy under Contract DE-AC02-09CH11466.

Princeton Plasma Physics Laboratory
Report Disclaimers

Full Legal Disclaimer

This report was prepared as an account of work sponsored by an agency of the United States Government. Neither the United States Government nor any agency thereof, nor any of their employees, nor any of their contractors, subcontractors or their employees, makes any warranty, express or implied, or assumes any legal liability or responsibility for the accuracy, completeness, or any third party's use or the results of such use of any information, apparatus, product, or process disclosed, or represents that its use would not infringe privately owned rights. Reference herein to any specific commercial product, process, or service by trade name, trademark, manufacturer, or otherwise, does not necessarily constitute or imply its endorsement, recommendation, or favoring by the United States Government or any agency thereof or its contractors or subcontractors. The views and opinions of authors expressed herein do not necessarily state or reflect those of the United States Government or any agency thereof.

Trademark Disclaimer

Reference herein to any specific commercial product, process, or service by trade name, trademark, manufacturer, or otherwise, does not necessarily constitute or imply its endorsement, recommendation, or favoring by the United States Government or any agency thereof or its contractors or subcontractors.

PPPL Report Availability

Princeton Plasma Physics Laboratory:

http://www.pppl.gov/techreports.cfm

Office of Scientific and Technical Information (OSTI):

http://www.osti.gov/scitech/

Related Links:

U.S. Department of Energy

U.S. Department of Energy Office of Science

U.S. Department of Energy Office of Fusion Energy Sciences

Adjoint method and runaway electron avalanche

Chang Liu
Princeton University, Princeton, New Jersey 08544, USA

Dylan P. Brennan
Princeton University, Princeton, New Jersey 08544, USA

Allen H. Boozer
Columbia University, New York, New York 10027, USA

Amitava Bhattacharjee
Princeton University, Princeton, New Jersey 08544, USA

Abstract.
The adjoint method for the study of runaway electron dynamics in momentum space [C. Liu, D.P. Brennan, A. Bhattacharjee, and A.H. Boozer, Phys. Plasmas 23, 010702 (2016).] is rederived using the Green's function method, for both the runaway probability function (RPF) and the expected loss time (ELT). The RPF and ELT obtained using the adjoint method are presented, both with and without the synchrotron radiation reaction force. The adjoint method is then applied to study the runaway electron avalanche. Both the critical electric field and the growth rate for the avalanche are calculated using this fast and novel approach.

Submitted to: *Plasma Phys. Control. Fusion*

1. Introduction

In plasma, a strong electric field can accelerate electrons to extremely high energy and form a "runaway" electron beam, due to the fact that the collisional friction force on an electron in the plasma decreases with the electron's velocity. Runaway electrons (REs) can be formed in various scenarios including solar flares [1], lighting in thunderstorms [2, 3], and magnetic confinement experiments like tokamaks [4–8] and reversed field pinches [9]. In tokamaks with large equilibrium current, runaway electrons can be produced in disruptions, due to the strong electric field formed in the thermal quench of the plasma. It is predicted that in a large tokamak device like the International Thermonuclear Experimental Reactor (ITER), a large population of REs can be produced and a large fraction of the plasma current will be transferred to be carried by the RE beam. The potential damage caused by these highly energetic electrons to the device poses a significant challenge for ITER to achieve its mission. It is therefore extremely important to have a profound understanding of the physics of runaway electrons, including their generation, acceleration and energy damping, and their interaction with various plasma modes in tokamaks, which can help inspire strategies for the prevention and mitigation of RE beams in disruptions.

The phenomena of "runaway" and the formed high energy tail distribution of electrons in momentum space has been well studied in both the unrelativistic case [10, 11] and the relativistic case [12]. Among the reported results, a very important finding is the so-called secondary runaway electron generation, or "runaway electron avalanche", which comes from a large angle scattering collision between an energetic runaway electron and a relatively low energy thermal electron. Although the large angle scattering event is rather rare, the growth caused by secondary generation is exponential and can become the dominant RE generation mechanism when a large population of REs has been generated. The physics model of secondary RE generation has recently been improved [13] to include the energy and pitch angle distribution of the seed runaway electrons. It has also been found that the pitch angle scattering effect and the trapping effect brought by the toroidicity can strongly affect the avalanche growth rate [14]. In addition, for highly relativistic runaway electrons the radiation reaction force becomes substantial and even comparable to the electric field force. The radiation of relativistic runaway electrons include synchrotron radiation [15–17], bremsstrahlung radiation [18–20], and Cerenkov radiation, all of which can affect electron dynamics in momentum space. As for the runaway electron avalanche, the radiation force can increase the critical electric field for avalanche to occur [21], and change the avalanche growth rate [22]. In addition, the stopping power can help form an "attractor" in the electron momentum space [15], which can lead to a bump-on-tail distribution [23].

To better understand these effects and the momentum-space structure of runaway electrons, we have developed an adjoint method [24], as reported in Ref. [25], to calculate two important functions in momentum space, the runaway probability function (RPF) and the expected loss time (ELT). In this paper, we show the application of the

adjoint method in RE avalanche calculation, and focus on runaway electron dynamics in momentum space. By adding the secondary generation source term into the kinetic equation and the adjoint equation, we can use the ELT and the RPF to calculate the critical electric field and the growth rate for the RE avalanche respectively. The adjoint method can be regarded as a "backward" method since the equation is similar to the kinetic equation of RE distribution function after a time-reversal transform. The adjoint method overcomes some shortcomings of the previous theoretical models such as the unphysical truncation of the diffusion term, and the calculation is much more efficient than the forward method such as directly solving the kinetic equation or Monte-Carlo simulation in obtaining the RPF and ELT. An adjoint kinetic equation can be derived in a few different ways, and one derivation appears in the Appendix of Ref. [25]. In the present paper, we present an alternative derivation of the adjoint method (denoted by "Green's function method") by using the Green's function of the kinetic equation to show the physical meaning of the adjoint kinetic equation solution, instead of the derivation in Ref. [25] (denoted by "SDE method") that is based on the relation between the stochastic differential equation (SDE) and the PDE through the Kolmogorov backwards equation. The two derivations are fundamentally equivalent.

This paper is organized as follows. In the Sec. 2 we introduce the homogeneous adjoint kinetic equation and its outcome, the runaway probability function, in both a general dynamical system and runaway electron momentum space. In the Sec. 3 we introduce the nonhomogeneous adjoint equation and the expected loss time, and use them to study the kinetics of runaway electrons affected by the synchrotron radiation reaction force. In Sec. 4 we discuss the application of the adjoint method to the RE avalanche, including how to calculate the critical electric field and the growth rate.

2. Homogeneous adjoint kinetic equation and the runaway probability function

2.1. Introduction to the runaway probability function

In this section we introduce the concept of the runaway probability function (RPF) in a general multi-dimensional stochastic dynamical system. We then prove that the RPF can be obtained as a solution of the homogeneous adjoint kinetic equation in the system, using the Green's function method instead of the SDE method in Ref. [25].

Consider a dynamical system where particles are moving in the phase space region Σ with boundary $\partial\Sigma$ and coordinates $\mathbf{x}$ ($\mathbf{x}$ may refer to both the particle's location in real space and its momentum). We can artificially split the boundary $\partial\Sigma$ into two parts, the runaway boundary $\partial\Sigma_1 \subset \partial\Sigma$, and the non-runaway boundary (or slowing-down boundary) $\partial\Sigma_2 = \partial\Sigma - \partial\Sigma_1$. The runaway probability function $P(\mathbf{x})$ is defined as a scalar function on Σ, which is the probability for a particle that initially lies at the location $\mathbf{x}$ to eventually leave the region Σ through the boundary $\partial\Sigma_1$. For a deterministic system P will be either zero or one, but for a stochastic system due to the

randomness of the particle's trajectory, P can have a value between zero and one.

The kinetic equation of the dynamical system, which describes the evolution of the particle distribution function f in Σ, can be written as

$$\frac{\partial f}{\partial t} = -\nabla \cdot \mathbf{U} + \sigma(\mathbf{x}), \tag{1}$$

where $\sigma(\mathbf{x})$ is the particle source, and $\mathbf{U}$ is the particle flow in phase space,

$$\mathbf{U} = \mathbf{v} f - \nabla \cdot (\mathsf{D} f)\,. \tag{2}$$

The two terms on the right hand side of Eq. (2) correspond to the advection and diffusion effects, respectively. Eq. (1) without the source term is also called the Fokker-Planck equation. We can further define the kinetic operator based on Eq. (1),

$$\hat{L}[f] = \nabla \cdot \mathbf{U} = \nabla \cdot (\mathbf{v} f) - \nabla\nabla : (\mathsf{D} f)\,, \tag{3}$$

the Green's function F of the kinetic operator $\hat{L}$, which satisfies

$$\hat{L}[F(\mathbf{x};\mathbf{x}_0)] = \delta(\mathbf{x} - \mathbf{x}_0), \tag{4}$$

and the homogeneous boundary condition ($F(\mathbf{x} \in \partial\Sigma; \mathbf{x}_0) = 0$). Note that F is a function independent of time. The physical meaning of F is a steady-state distribution function formed by a unit particle source at $\mathbf{x} = \mathbf{x}_0$ and particles are allowed to leave the system at the boundaries.

We now define the adjoint operator. For any given functional operator $\hat{L}$, its adjoint operator $\hat{L}^\dagger$ fulfills,

$$\int g \hat{L}[f] d\mathbf{x} = \int f \hat{L}^\dagger[g] d\mathbf{x}, \tag{5}$$

where f and g are two arbitrary functions. Note that the integral is calculated over the whole phase space rather than being limited to Σ. For the kinetic operator $\hat{L}$ in Eq. (3), the corresponding adjoint operator $\hat{L}^\dagger$ is

$$\hat{L}^\dagger[g] = -\mathbf{v} \cdot \nabla g - \mathsf{D} : \nabla\nabla g. \tag{6}$$

Introduce another function G in Σ that satisfies the homogeneous adjoint kinetic equation,

$$\hat{L}^\dagger[G] = 0. \tag{7}$$

Different from F, the boundary condition for G is a nonhomogeneous one given by the runaway-slowing-down separation of the boundary,

$$G(\mathbf{x} \in \partial\Sigma_1) = 1, \quad G(\mathbf{x} \in \partial\Sigma_2) = 0. \tag{8}$$

We can now prove that G is equal to the RPF P. To do that, we can combine the above equations that are satisfied by $F(\mathbf{x};\mathbf{x}_0)$ and G together to find the relations between them. Calculate the following integral,

$$\int_\Sigma G \hat{L}[F] d\mathbf{x} = \int_{\partial\Sigma} (G\mathbf{U} + \mathsf{D} \cdot \nabla G F) \cdot \mathbf{n} da + \int_\Sigma F \hat{L}^\dagger[G] d\mathbf{x}, \tag{9}$$

where $\mathbf{U}$ is the phase space particle flow associated with $F(\mathbf{x};\mathbf{x}_0)$, $\int ...da$ is the integral on the boundary $\partial\Sigma$, and $\mathbf{n}$ is the unit vector normal to the boundary. Applying Eqs. (4) (7) and the boundary conditions for F and G, we obtain

$$G(\mathbf{x}=\mathbf{x}_0)=\int_{\partial\Sigma_1}\mathbf{U}\cdot\mathbf{n}da. \tag{10}$$

Thus $G(\mathbf{x}_0)$ equals the total particle flow of $F(\mathbf{x};\mathbf{x}_0)$ that comes out of the system at boundary $\partial\Sigma_1$. Note that $\int_{\partial\Sigma}\mathbf{U}\cdot\mathbf{n}da=1$ according to the conservation of particle density, therefore $G(\mathbf{x}_0)$ also represents the probability for a particle to run out of the system at boundary $\partial\Sigma_1$ rather than $\partial\Sigma_2$, if it was initially injected at $\mathbf{x}=\mathbf{x}_0$. Comparing with the definition of RPF, we obtain $G=P$.

Note that in Ref. [25], we used the SDE method to show that the RPF satisfies the homogeneous adjoint equation. In that proof we showed clearly that the adjoint method is a "backwards" method, since it calculates the value of P at any location $\mathbf{x}$ by summing P of all the possible next-step locations of $\mathbf{x}$ (An equivalent approach to obtain the result is to solve the Backward Stochastic Differential Equation (BSDE) [26]. Because we already know the values of P at the boundaries, we can then calculate P in the whole region Σ by tracing backwards in time, which turns out to be equivalent to solving the adjoint equation.) On the other hand, for the "forward" methods including solving Eq. (4) to calculate the Green's function or doing Monte-Carlo simulation for the forward SDE, to get the RPF in Σ one needs to do the calculation for every location separately. Therefore, the adjoint method is a more efficient approach to obtain the RPF.

2.2. Runaway probability function in electron momentum space

We now apply the adjoint method to runaway electrons. Consider relativistic runaway electrons that are driven by a uniform and constant electric field, the kinetic equation describing the electron distribution function evolution in momentum space can be written as

$$\frac{\partial f}{\partial\hat{t}}+E[f]+C[f]=0, \tag{11}$$

where

$$E[f]=\frac{1}{p^2}\frac{\partial}{\partial p}\left[p^2\hat{E}f\right]+\frac{\partial}{\partial\xi}\left[\frac{1-\xi^2}{p}\hat{E}f\right], \tag{12}$$

$$C[f]=-\frac{1}{p^2}\frac{\partial}{\partial p}\left[\left(1+p^2\right)f\right]-\frac{Z+1}{2}\frac{\sqrt{1+p^2}}{p^3}\frac{\partial}{\partial\xi}\left[(1-\xi^2)\frac{\partial f}{\partial\xi}\right], \tag{13}$$

describe the electric field force and the collisional operator, respectively. Here p is the electron momentum (normalized to mc, m is the electron mass and c is the speed of light), ξ is the cosine of the pitch angle $\xi=p_\parallel/p$, Z is the ion effective charge, $\hat{E}=E/E_{\mathrm{CH}}$ where E_{CH} is the Connor-Hastie critical electric field [12] $E_{\mathrm{CH}}=n_e e^3\ln\Lambda/\left(4\pi\epsilon_0^2 m_e c^2\right)$ and $\ln\Lambda$ is the Coulomb logarithm, and $\hat{t}=t/\tau$ where τ is the relativistic electron collision time $\tau=m_e c/\left(eE_{\mathrm{CH}}\right)$. Note that in the kinetic equation

the phase angle ϕ is ignored and the momentum space is reduced to be 2D, assuming that electrons are moving in a strong magnetic field and the phase angle dependence of f can be averaged out. We also ignore the trapping effect brought by the toroidicity, making the results relevant to REs that are close to the magnetic axis. For simplicity, the radiation reaction force in ignored in this section, but will be addressed in the following sections.

We now study the dynamics of an electron guided by the Eq. (11) in a chosen region of momentum space, $p \in (p_{\min}, p_{\max})$, and $\xi \in (-1, 1)$. $p_{\min}$ and $p_{\max}$ are two boundaries in momentum space that are located far from the runaway-slowing-down transition region (The solution is checked to be insensitive to the boundary locations). We define $p = p_{\max}$ as the "runaway boundary", and any electron that reaches this boundary as a "runaway electron". The $p = p_{\min}$ is then defined as the slowing-down boundary. The runaway probability function, $P(p_0, \xi_0)$, means the probability for an electron initially at (p_0, ξ_0) to eventually reach p_{max} and leave the region. As discussed before, P satisfies the homogeneous adjoint equation,

$$\mathcal{E}\left[P\right] + \mathcal{C}\left[P\right] = 0, \tag{14}$$

where

$$\mathcal{E}\left[P\right] = -\hat{E}\left[\xi\frac{\partial P}{\partial p} + \frac{1-\xi^2}{p}\frac{\partial P}{\partial \xi}\right], \tag{15}$$

$$\mathcal{C}\left[P\right] = \frac{1+p^2}{p^2}\frac{\partial P}{\partial p} - \frac{Z+1}{2}\frac{\sqrt{1+p^2}}{p^3}\frac{\partial}{\partial \xi}\left[(1-\xi^2)\frac{\partial P}{\partial \xi}\right] \tag{16}$$

The boundary conditions of P are $P(p = p_{\min}, \xi) = 0, \quad P(p = p_{\max}, \xi) = 1$.

We solve Eq. (14) numerically using a finite difference representation on p and a Legendre polynomial representation on ξ, which is similar to the numerical representation used in CODE [27], to obtain the RPF. The solution is calculated using MATLAB sparse matrix solver. Fig. 1 shows two solutions of the RPF in the momentum space, for both $Z = 1$ and $Z = 7$. The solution of P is separated into three regions. For small momentum P is close to zero, which means particles will almost definitely slow down and return the thermal electron population. For large momentum P is close to one, which means electrons will have a high probability to run away. There is a transition region between these two regions, which characterizes the critical runaway momentum p_{crit}. Note that p_{crit} increases with the pitch angle θ. Comparing the two cases with different Z, we can find that p_{crit} also increases with Z or the pitch angle scattering effect. This is because in the model the electric field only accelerates an electron in the direction parallel to the magnetic field, so an electron with larger initial pitch angle or experiencing stronger pitch angle scattering is less likely to run away.

The runaway-slowing-down separatrix calculated using the test particle method in Ref. [28] is also shown for reference. Note that the separatrix lies in the transition region of P, which reflects the agreement of the two methods. However, the adjoint method provides a smooth RPF that changes gradually from 0 to 1 rather than a step

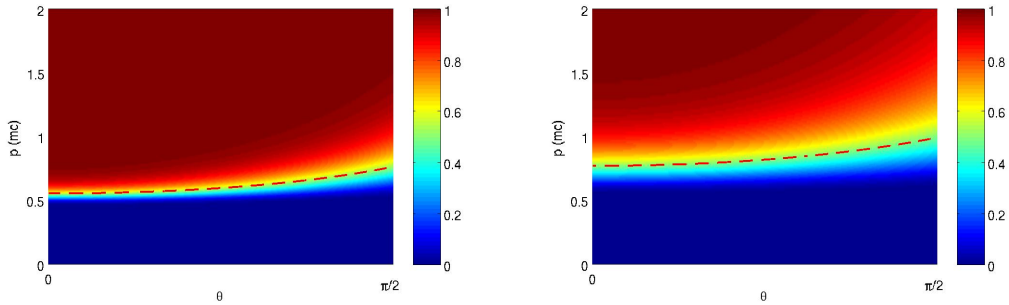

Figure 1. The profile of RPF for $E = 6E_{\mathrm{CH}}$, $Z = 1$ (left) and $Z = 7$ (right). θ is the pitch angle. The red dashed line is the separatrix calculated using the test particle method in Ref. [15].

function. The width of the transition region depends on the amplitude of the pitch angle scattering term, which increases with Z. In addition, for the $Z = 7$ case we can see clearly from Fig. 1 that the transition region is not symmetric at two sides of the separatrix, which is wider on the high momentum side. All these traits of the transition region are not captured in the test particle method, which ignores the diffusion effect in the pitch angle scattering.

Fig. 2 shows the value of P as a function of p for $\xi = 1$ in the transition region. The result is benchmarked with a Monte-Carlo simulation, which is achieved by sampling a large number of electrons that start at one initial position and follow the stochastic differential equation (SDE) that corresponds to Eq. (11). We then count the electrons that hit the low and high energy boundaries after a certain time. The two results are close. Note that unlike the Monte-Carlo method which takes significant computer time, the adjoint method is fast and only requires solving the PDE once to obtain the RPF.

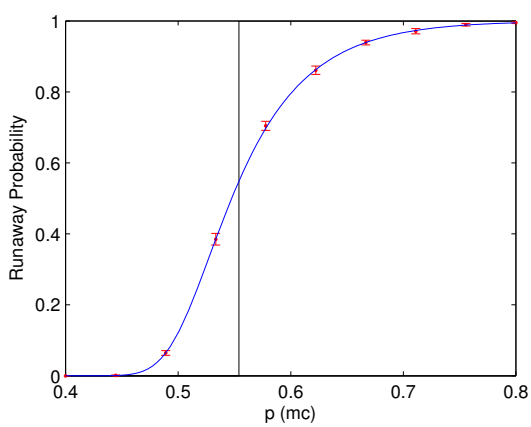

Figure 2. P for $Z = 1$ and $E = 6E_{\mathrm{CH}}$ at $\xi = 1$ near the transition region. The red dots and error bars reflect the mean and the variation of the Monte-Carlo simulation results. The black vertical line shows the crossing point of the separatrix calculated using the test-particle method at $\xi = 1$.

Apart from separating different regions in the RE momentum space and finding

the value of $p_{\rm crit}$, the RPF can also be useful for solving various RE problems. For example, when combined with the secondary RE generation source term, the RPF can help estimate the avalanche growth rate, which will be discussed in Sec. 4. In addition, the RPF can be used to determine the number of seed runaway electrons produced through the slide away of the thermal electron Maxwellian tail in the thermal quench, which will strongly affect the number of RE avalanche e-folds and the conversion ratio from plasma current to RE current in the current quench. This will be addressed in future work.

3. Nonhomogeneous adjoint kinetic equation and the expected loss time

3.1. Introduction to the expected loss time

The adjoint method can also be used to study the stochastic dynamical system with an attractor. Note the runaway probability function gives the information of a particle's final destination regardless of the time it takes to reach it. Considering that we are studying a dynamical system including an attractor formed by the advection forces, e. g. the runaway electron momentum space with a radiation reaction force [15] (including both synchrotron radiation and bremsstrahlung radiation), then the attractor will affect the particle's trajectory and significantly increase the time for it to reach the boundary. However, the RPF is not the best way to describe this change since it does not have information about loss time. To overcome this issue, we introduce another function of phase space, the expected loss time (ELT). We now show the derivation of the ELT using the Green's function method.

Following the definition of the Fokker-Planck operator $\hat{L}$ and the adjoint operator $\hat{L}^\dagger$, we define function T to satisfy the nonhomogeneous adjoint equation,‡

$$\hat{L}^\dagger[T] = 1 \tag{17}$$

with the homogeneous boundary condition $T(\mathbf{x} \in \partial\Sigma) = 0$.

To show the connection between T and the Green's function $F(\mathbf{x};\mathbf{x}_0)$, we calculate the following integral,

$$\int_\Sigma \hat{L}[F]T d\mathbf{x} = \int_{\partial\Sigma} (T\mathbf{U} + \mathsf{D}\cdot\nabla TF)\cdot\mathbf{n}da + \int_\Sigma F\hat{L}^\dagger[T]d\mathbf{x}. \tag{18}$$

Applying Eqs. (4) (17) and the boundary conditions for $F(\mathbf{x};\mathbf{x}_0)$ and T, we obtain

$$T(\mathbf{x}=\mathbf{x}_0) = \int_\Sigma F d\mathbf{x}. \tag{19}$$

Thus T is equal to the integral of the Green's function F in Σ, or the total number of particles N in $F(\mathbf{x};\mathbf{x}_0)$. Recall the $F(\mathbf{x};\mathbf{x}_0)$ is the steady state distribution function formed by the unit source $\delta(\mathbf{x}-\mathbf{x}_0)$, the rate for each particle to leave the system is then $1/N$. Therefore we prove that T also represents the expected time for a particle initially at $\mathbf{x}=\mathbf{x}_0$ to leave the system at boundaries.

‡ In Ref. [25] we use -1 on the right hand side of the nonhomogeneous adjoint Fokker-Planck equation, because the adjoint operator defined in Re. [25] is the opposite of the adjoint operator in this paper.

Similar to the RPF, the ELT can also be obtained from the "forward" method by calculating the Green's function $F(\mathbf{x};\mathbf{x}_0)$ or by doing Monte-Carlo simulation for every location in Σ. But the adjoint method provides a much more efficient approach.

3.2. Synchrotron radiation reaction force and expected loss time for runaway electrons

With the help of the expected loss time, we can now study the dynamics of runaway electrons in the presence of the radiation force. In this paper we will only focus on the synchrotron radiation reaction force (SRRF), which is calculated by doing a gyro-average of the Abraham-Lorentz-Dirac (ALD) force [29]. In tokamaks the SRRF can come both from electrons' gyro motion due to the magnetic field and electrons' toroidal motion following field lines. However, for electrons with energy below 20MeV, the SRRF from from the gyro motion far exceeds that from the toroidal motion. Thus in this paper we only consider the SRRF from gyro motion.

The kinetic equation including the SRRF is

$$\frac{\partial f}{\partial \hat{t}} + E[f] + C[f] + R[f] = 0, \tag{20}$$

where

$$R[f] = \frac{1}{\hat{\tau}_r}\left\{-\frac{1}{p^2}\frac{\partial}{\partial p}\left[p^3\gamma(1-\xi^2)f\right] + \frac{\partial}{\partial \xi}\left[\frac{1}{\gamma}\xi(1-\xi^2)f\right]\right\}, \tag{21}$$

and $\hat{\tau}_r = \tau_r/\tau$. τ_r is the timescale for the SRRF energy loss $\tau_r = 6\pi\epsilon_0 m_e^3 c^3/\left(e^4 B^2\right)$.

Define $T(p_0,\xi_0)$ as the expected time for an electron initially at (p_0,ξ_0) to reach the low energy boundary $p_{\min}$ or the high energy boundary $p_{\max}$. Note that $1/T = 1/T_s + 1/T_r$, where T_s is the expected slowing down time and T_r is the expected runaway time. The ratio of the two terms is $(1-P)/P$. As discussed before, T satisfies the nonhomogeneous adjoint kinetic equation. The adjoint kinetic equations for P and T including SRRF can be written as

$$\mathcal{E}\left[P\right] + \mathcal{C}\left[P\right] + \mathcal{R}\left[P\right] = 0, \quad \mathcal{E}\left[T\right] + \mathcal{C}\left[T\right] + \mathcal{R}\left[T\right] = 1, \tag{22}$$

where

$$\mathcal{R}\left[P\right] = \frac{1}{\hat{\tau}_r}\left[\gamma p(1-\xi^2)\frac{\partial P}{\partial p} - \frac{1}{\gamma}\xi(1-\xi^2)\frac{\partial P}{\partial \xi}\right]. \tag{23}$$

The boundary condition for T is homogeneous, $T(p=p_{\min},\xi) = T(p=p_{\max},\xi) = 0$.

In the following discussion we will show how the SRRF affects the runaway electron dynamics using the ELT in two different scenarios. We first focus on the case that $E \gg E_c$, which means that the runaway process (electron leaves the region through the $p_{\max}$ boundary) can still happen. We find that in this case after adding the SRRF, the solution of RPF is not very different from the non-radiation case (An example is shown in Ref. [25].). This means that in this scenario, unlike the pitch angle scattering, the SRRF will not much affect the location or the width of the transition region in RPF.

Nevertheless, the SRRF can significantly increase the ELT in the high energy regime. Fig. 3 shows the results of T for $E = 3E_{\mathrm{CH}}$ and 3 different values of $\hat{\tau}_r$. We

can see that as the SRRF becomes stronger ($\hat{\tau}_r$ becomes smaller), the ELT in the region beyond the separatrix increases. This is because in the high energy region the SRRF can strongly dissipate electron energy, and thereby slow down the runaway process. In addition, for the strong radiation case ($\hat{\tau} = 2$), T becomes almost flat in the high energy region. This indicates the existence of an attractor formed by the balance of the three forces in Eq. (20), and all electrons in the high energy region will first accumulate near the attractor, and thus have a similar value of ELT.

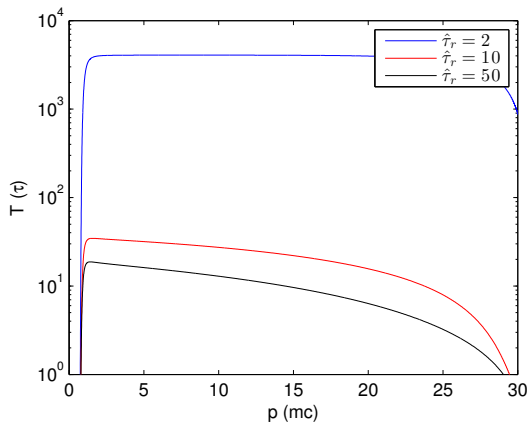

Figure 3. The expected loss time at $\xi = 1$ for $E = 3E_{\mathrm{CH}}$, $Z = 1$ and 3 different values of $\hat{\tau}_r$ in the $E \gg E_c$ scenario.

We then look at the scenario with strong SRRF and $E < E_c$. In this case electrons can no longer run away as the electric force is subdominant compared to the sum of the collisional force and the SRRF in the whole momentum space. The RPF will be zero in almost the whole momentum space except for a narrow region near $p_{\max}$ boundary, thus $T_r \to \infty$ and $T \approx T_s$. In other words, the ELT now characterizes the expected time for an existing high energy electron to lose its energy and slow down to the thermal electron population.

Figure 4 shows the calculated $T(p, \xi)$ at $\xi = 1$ for $E = 1.5E_{\mathrm{CH}}$ and 3 different values of $\hat{\tau}_r$. We see that in this case T is a monotonically increasing function of p. Among these results a very interesting example is $\hat{\tau}_r = 20$, in which E is smaller than but very close to E_c (the marginal case). In the marginal case, T has a prompt jump between the low and high energy regions. This is because in the marginal case the sum of the collisional force and the SRRF dominates the electric force in the whole momentum space except for a region near p_{crit}, where all the forces reach a balance and the dynamics of electron is dominated by diffusion. Thus electrons that reach this region will take a long time to cross it through random walk, which is similar to a potential barrier in the electron momentum dissipation path. If the SRRF is larger and $E \ll E_c$, this jump becomes smaller or non-existent because the strong radiation force makes this region advection dominant.

The ELT can be applied to estimate the runaway electron beam decay time in experiments, and help explain the runaway electron population hysteresis and

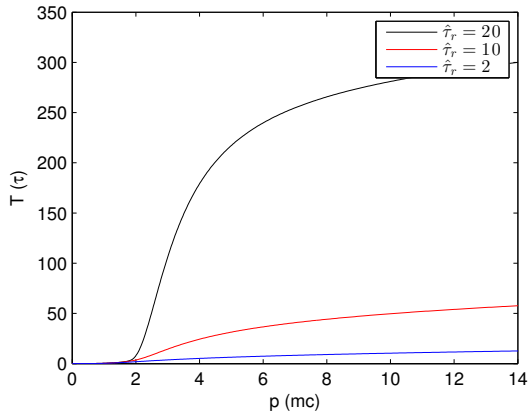

Figure 4. The expected loss time at $\xi = 1$ for $E = 1.5E_{\mathrm{CH}}$, $Z = 1$ and 3 different values of $\hat{\tau}_r$ in the $E < E_c$ scenario.

distribution. In both the quiescent runaway electron experiments (QRE) and disruption experiments, due to the decreasing magnitude of E/E_c, the runaway electron beam will have a transition from growth to decay. This means that at the beginning of the decay, there is already a population of high energy electrons formed by previous growth. The expected slowing-down time for these electrons determines the timescale for decay. The result of the ELT in the marginal case shows that if E is very close to E_c, the RE decay can be very slow. This can contribute to a hysteresis effect [21] for the runaway electron population when the electric field is ramped up and down. In addition, the marginal case ELT indicates very fast decay of the electrons with $p < p_{\mathrm{crit}}$ and much slower decay of the higher energy electrons, which will result in a bump-on-tail electron distribution in the momentum space near p_{crit}. This non-monotonic electron distribution has been observed in experiments in the post-disruption case [30]. However, this effect will be weakened by the secondary RE generation, which will be discussed below.

4. Runaway electron avalanche

In this section we focus on the secondary runaway electron generation, which comes from the large angle scattering of a low-energy thermal electron by a high-energy relativistic electron. It has been shown in the Rosenbluth-Putvinski [31] model that the secondary runaway electron generation can cause an exponential growth of the runaway electron population, or "runaway electron avalanche". Here we show the applications of the runaway probability function and the expected loss time on the runaway electron avalanche study.

The kinetic equation for relativistic electron including the secondary generation can be written as

$$\frac{\partial f}{\partial \hat{t}} + E[f] + C[f] + R[f] = S[f], \tag{24}$$

where S is the source term describing the secondary runaway electron generation. Using

the model from Ref. [13], S can be expressed as

$$S[f](p,\xi) = \frac{1}{p^2}\int \mathsf{S}(p_e,\xi_e,p,\xi)f(p_e,\xi_e)p_e^2 dp_e d\xi_e. \tag{25}$$

The function $\mathsf{S}(p_e,\xi_e,p,\xi)$ is the scattering probability function, describing the rate of change of the number of electrons at momentum (p,ξ) due to large angle collisions with electrons at (p_e,ξ_e). $\mathsf{S}(p_e,\xi_e,p,\xi)$ is derived from the Møller cross section, which can be regarded as the relativistic version of the Coulomb cross section. In this model we have taken into account the energy and pitch angle distribution of the seed runaway electrons, which is an improvement over the Rosenbluth-Putvinski model. Note that although the scattering probability function S is complicated and depends on both p and ξ, it can be remarkably simplified by using a Legendre polynomial representation of ξ, which is the representation used in CODE and what we are using in solving the adjoint kinetic equations.

We first use the nonhomogeneous adjoint kinetic equation to calculate the critical electric field, E_c, for runaway electron avalanche. Classical theory predicts that $E_c = E_{\mathrm{CH}}$, and the avalanche growth rate is almost a linear function of $E - E_{\mathrm{CH}}$. However, recent studies show that the SRRF can increase E_c due to the additional energy dissipation. The kinetic equation Eq. (24) yields the nonhomogeneous adjoint equation including the secondary generation,

$$\mathcal{E}\left[\bar{T}\right] + \mathcal{C}\left[\bar{T}\right] + \mathcal{R}\left[\bar{T}\right] - \mathcal{S}\left[\bar{T}\right] = 1, \tag{26}$$

where

$$\mathcal{S}\left[\bar{T}\right](p,\xi) = \int \mathsf{S}(p,\xi,p',\xi')\bar{T}(p',\xi')dp'd\xi'. \tag{27}$$

The solution $\bar{T}$ of the adjoint equation Eq. (26) also corresponds to the integral of the Green's function of the kinetic equation Eq. (24). However, since Eq. (24) is not a density conserving equation (It contains a particle source term.), the solution $\bar{T}$ is not the expected time for one single electron to leave the region of interest anymore. Instead, it corresponds to the sum of the expected loss time of the test particle and the loss time of all the children particles born by it through the source term Eq. (24). The expected time for the electron population to decay will be shorter than $\bar{T}$ since the electrons will dissipate energy simultaneously.

The result of $\bar{T}$ is very useful to study the runaway electron avalanche. To show that, we calculate $\bar{T}$ for $Z = 1, \hat{\tau}_r = 2$ and different E/E_{CH}, which is shown in Fig. 5. We find that, as electric field increases, the value of $\bar{T}$ above the critical momentum increases significantly. Moreover, when E/E_{CH} is above a certain threshold, the value of $\bar{T}$ in the high momentum region jumps to infinity. This means that in this case the newly generated secondary runaway electrons will sustain the electron population in the high energy region, and the RE population in this region will never deplete. In other words, the avalanche is happening.

In Ref. [25], we found that when taking into account the energy decay due to the large angle scattering by replacing the Landau-Fokker-Planck collision operator in

the adjoint equation with the Boltzmann collision operator, the result of ELT in the marginal case can decrease significantly. This is because the large angle scattering can help high energy electrons pass the potential barrier in momentum space and thus reduce the time spent in the energy decay. However, when including the source term for secondary generation, the difference brought by the Boltzmann collision operator becomes very small. This means that the additional energy dissipation from large angle scattering in the marginal case will be overwhelmed by the secondary RE generation effect, and thus is not important.

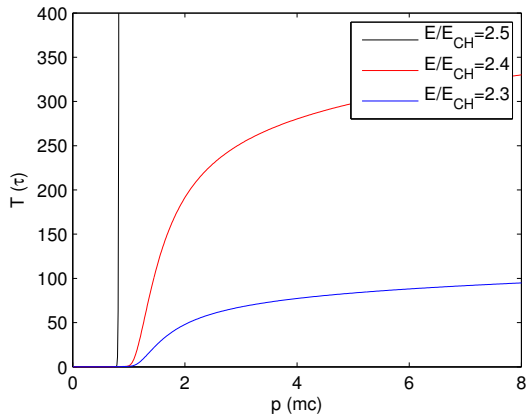

Figure 5. $\bar{T}$ calculated using Eq. (26) at $\xi = 1$ for $Z = 1$, $\hat{\tau}_r = 2$ and three values of $E/E_{\rm CH}$.

We can thus use the condition of $\bar{T} \to \infty$ as a criterion for the runaway electron avalanche, and determine the critical electric field E_c. By scanning the electric field from low to high for different parameters of $\hat{\tau}_r$ and Z, we can determine the dependence of E_c on these two parameters, as shown in Fig. 6. We also compare the results with the critical electric field calculated using an approximate analytical distribution function [21]. The two results are very close for small Z cases, and for large Z the E_c calculated using the adjoint method is smaller than that from the analytical method§.

Note that in experiments a critical electric field larger than $E_{\rm CH}$ has been observed, but even taking SRRF into account, the calculated E_c is still smaller than the observation. Two possible reasons have been posed to explain the discrepancy. The first is that for a small electric field the critical momentum $p_{\rm crit}$ for an electron to run away is very high, which results in an extremely slow growth that is hard to observe. Another explanation about the observed critical electric field corresponding to the turning point of the Hard X-ray signal in the QRE experiments [32] relies on the energy dependence of the diagnostic and the redistribution of runaway electrons in momentum space [33] with a dropping E/E_c. In addition, other kinetic effects such as the kinetic instabilities [34–36] and magnetic field fluctuation [37] may also play a role.

§ Note that the result of E_c is different from the result in Ref. [25], where a different criterion based on the transition region in RPF is used. The criterion used here has a clearer physics meaning and is more relevant to the RE avalanche.

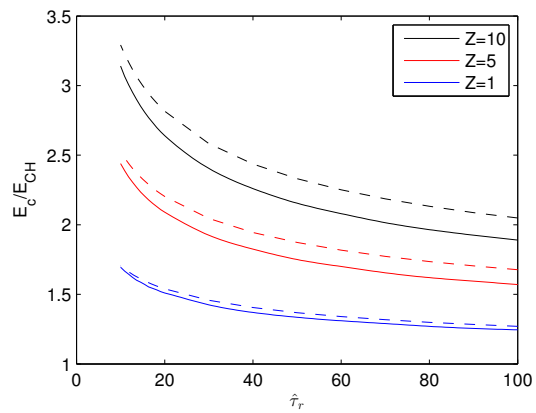

Figure 6. The critical electric field for avalanche E_c calculated using the adjoint method (solid line) plotted as a function of $\hat{\tau}_r$ for various Z. E_0 from Ref. [21] (dashed line) plotted for comparison.

On the other hand, the RPF can be utilized to calculate the avalanche growth rate. For a given runaway electron distribution, we can calculate the distribution of the secondary runaway electrons generated using Eq. (25). However, the calculated $S(p,\xi)$ is a divergent function for $p \to 0$. To know how many of the newly generated electrons can run away, we must use the RPF calculated using Eq. (22) (without the source term). The avalanche growth rate is then

$$\gamma = \frac{1}{n_r}\int S(p,\xi)P(p,\xi)p^2 dp d\xi, \tag{28}$$

where n_r is the density of the existing runaway electrons‖. Note that for a runway tail whose growth is dominated by the avalanche, the exponential growth rate at every part of the momentum space is almost the same, which means that the distribution function is growing exponentially whereas the shape does not change. In this case we can calculate the shape of the runaway electron tail distribution by specifying γ,

$$-E[f] - C[f] - R[f] + S[f] = \frac{\partial f}{\partial t} \approx \gamma f. \tag{29}$$

Thus for a given γ, f can be calculated as an eigenvector. Eqs. (28-29) provide an iterative approach to calculate the avalanche growth rate and the shape of the distribution function of the runaway electron tail. Fig. 7 shows the calculated avalanche growth rate using this method. We also show a benchmark with the results obtained from a kinetic simulation by solving Eq. (24) using CODE. The two results are very close.

5. Summary

The adjoint kinetic equation is derived and applied to calculate the runaway probability and the expected loss time regarding runaway electron dynamics in momentum space.

‖ n_r can be calculated by integrating the RE distribution function from the critical momentum to the high energy boundary. The critical momentum is chosen as $P(p_{\rm crit}, \xi = 1) = 0.5$.

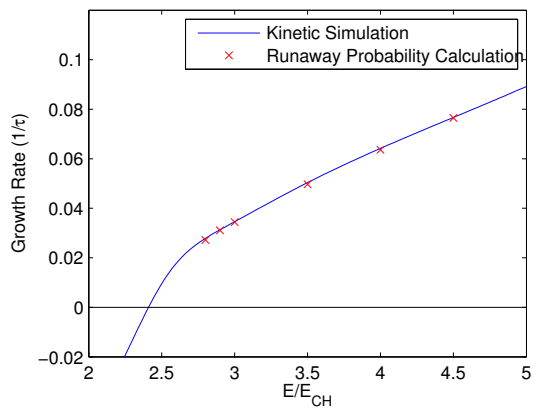

Figure 7. The growth or decay rate of high energy electron population as a function E/E_{CH} for $Z = 1$ and $\hat{\tau}_r = 2$. τ is the relativistic electron collision time $\tau = m_e c/\left(eE_{\mathrm{CH}}\right)$. The Coulomb logarithm $\ln\Lambda$ is set to be 20 due to the high velocity of REs. The blue line is the obtained by solving Eq. (24) directly using CODE. The red dots are the results obtained using the RPF and iterative method. Each point is calculated using 10 iterations. The positive value corresponds to the avalanche growth rate, and the negative value corresponds to the decaying rate of high energy electron population for $E < E_c$.

The runaway probability function successfully identifies the runaway-slowing-down separatrix, and the increase of the critical momentum induced by the pitch angle scattering effect. The expected loss time shows the existence of an attractor in the runaway electron momentum space from the synchrotron radiation reaction force. Analysis of the ELT in the marginal case reveals a potential barrier near the critical runaway momentum. In addition, both quantities are utilized to study the runaway electron avalanche, and provide an accurate approach to calculate the critical electric field and the avalanche growth rate.

The adjoint method can also be easily extended to study the influences of other physics on runaway electron dynamics, including Bremsstrahlung radiation [18, 20] and magnetic fluctuations [37], by adding the corresponding operators into the adjoint kinetic equation. Other areas of runaway electron physics can also be studied, such as the thermal quench where RPF can help determine the number of seed REs generated. In addition, the adjoint method can be used to study any stochastic dynamical system that has a separatrix or a singular point, e.g. particle behavior close to the magnetic separatrix and the X-point. Future applications of this method are promising.

Acknowledgments

We thank D. del-Castillo-Negrete, O. Embréus, I. Fernández-Gómez, N. Fisch, T. Fülöp, P. Helander, E. Hirvijoki, J. Krommes, G. Papp, A. Stahl, G. Zhang and Y. Zhou for useful discussions. The numerical calculations are conducted on the PPPL Beowulf cluster. This work is supported by the U.S. Department of Energy under Contract

DE-AC02-09CH-11466 and DE-FG02-03ER54696.

References

[1] Holman G D 1985 *Astrophys. J.* **293** 584

[2] Wilson C T R 1924 *Proc. Phys. Soc. London* **37** 32D

[3] Gurevich A V, Milikh G M and Roussel-Dupre R 1992 *Phys. Lett. A* **165** 463–468

[4] Knoepfel H and Spong D A 1979 *Nucl. Fusion* **19** 785

[5] Kwon O J, Diamond P H, Wagner F, Fussmann G, Team A and Team N I 1988 *Nucl. Fusion* **28** 1931

[6] Gill R D 1993 *Nucl. Fusion* **33** 1613

[7] Jaspers R, Cardozo N J L, Schuller F C, Finken K H, Grewe T and Mank G 1996 *Nucl. Fusion* **36** 367

[8] Helander P, Eriksson L G and Andersson F 2002 *Plasma Phys. Control. Fusion* **44** B247

[9] O'Connell R, Hartog D J D, Forest C B, Anderson J K, Biewer T M, Chapman B E, Craig D, Fiksel G, Prager S C, Sarff J S, Terry S D and Harvey R W 2003 *Phys. Rev. Lett.* **91** 045002

[10] Dreicer H 1959 *Phys. Rev.* **115** 238–249

[11] Kruskal M D and Bernstein I B 1964 *Phys. Fluids* **7** 407–418

[12] Connor J W and Hastie R J 1975 *Nucl. Fusion* **15** 415

[13] Boozer A H 2015 *Phys. Plasmas* **22** 032504

[14] Nilsson E, Decker J, Peysson Y, Granetz R S, Saint-Laurent F and Vlainic M 2015 *Plasma Phys. Control. Fusion* **57** 095006

[15] Martín-Solís J R, Alvarez J D, Sánchez R and Esposito B 1998 *Phys. Plasmas* **5** 2370–2377

[16] Andersson F, Helander P and Eriksson L G 2001 *Phys. Plasmas* **8** 5221–5229

[17] Stahl A, Hirvijoki E, Decker J, Embréus O and Fülöp T 2015 *Phys. Rev. Lett.* **114** 115002

[18] Bakhtiari M, Kramer G J, Takechi M, Tamai H, Miura Y, Kusama Y and Kamada Y 2005 *Phys. Rev. Lett.* **94** 215003

[19] Fernández-Gómez I, Martín-Solís J R and Sánchez R 2012 *Phys. Plasmas* **19** 102504

[20] Embréus O, Stahl A and Fülöp T 2016 *arXiv:1604.03331*

[21] Aleynikov P and Breizman B N 2015 *Phys. Rev. Lett.* **114** 155001

[22] Martín-Solís J R, Sánchez R and Esposito B 2000 *Phys. Plasmas* **7** 3814–3817

[23] Hirvijoki E, Pusztai I, Decker J, Embréus O, Stahl A and Fülöp T 2015 *J. Plasma Phys.* **81** 475810502

[24] Karney C F F and Fisch N J 1986 *Phys. Fluids* **29** 180–192

[25] Liu C, Brennan D P, Bhattacharjee A and Boozer A H 2016 *Phys. Plasmas* **23** 010702

[26] Zhao W, Zhang W and Zhang G 2015 *arXiv:1412.7821*

[27] Landreman M, Stahl A and Fülöp T 2014 *Comp. Phys. Comm.* **185** 847–855

[28] Parks P B, Rosenbluth M N and Putvinski S V 1999 *Phys. Plasmas* **6** 2523–2528

[29] Hirvijoki E, Decker J, Brizard A J and Embréus O 2015 *J. Plasma Phys.* **81** 475810504

[30] Reux C, Plyusnin V, Alper B, Alves D, Bazylev B, Belonohy E, Boboc A, Brezinsek S, Coffey I, Decker J, Drewelow P, Devaux S, Vries P C d, Fil A, Gerasimov S, Giacomelli L, Jachmich S, Khilkevitch E M, Kiptily V, Koslowski R, Kruezi U, Lehnen M, Lupelli I, Lomas P J, Manzanares A, Aguilera A M D, Matthews G F, Mlynář J, Nardon E, Nilsson E, Thun C P v, Riccardo V, Saint-Laurent F, Shevelev A E, Sips G, Sozzi C and Contributors J E T 2015 *Nucl. Fusion* **55** 093013

[31] Rosenbluth M N and Putvinski S V 1997 *Nucl. Fusion* **37** 1355

[32] Paz-Soldan C, Eidietis N W, Granetz R, Hollmann E M, Moyer R A, Wesley J C, Zhang J, Austin M E, Crocker N A, Wingen A and Zhu Y 2014 *Phys. Plasmas* **21** 022514

[33] Stahl A, Landreman M, Papp G, Hollmann E and Fülöp T 2013 *Phys. Plasmas* **20** 093302

[34] Parail V V and Pogutse O P 1978 *Nucl. Fusion* **18** 303

[35] Fülöp T, Pokol G, Helander P and Lisak M 2006 *Phys. Plasmas* **13** 062506

[36] Aleynikov P and Breizman B 2015 *Nucl. Fusion* **55** 043014

[37] Martín-Solís J R, Sánchez R and Esposito B 1999 *Phys. Plasmas* **6** 3925–3933

Princeton Plasma Physics Laboratory
Office of Reports and Publications

Managed by
Princeton University

under contract with the
U.S. Department of Energy
(DE-AC02-09CH11466)

P.O. Box 451, Princeton, NJ 08543
Phone: 609-243-2245
Fax: 609-243-2751

E-mail: publications@pppl.gov

Website: http://www.pppl.gov